

## First results on angular distributions of thermal dileptons in nuclear collisions

R. Amaldi,<sup>1</sup> K. Banicz,<sup>2,3</sup> J. Castor,<sup>4</sup> B. Chaurand,<sup>5</sup> C. Cicab,<sup>6</sup> A. Colla,<sup>1</sup> P. Cortese,<sup>1</sup> S. Damjanovic,<sup>2,3</sup> A. D'Amico,<sup>2,7</sup> A. de Falco,<sup>6</sup> A. Devaux,<sup>4</sup> L. Ducroux,<sup>8</sup> H. En'yo,<sup>9</sup> J. Fargeix,<sup>4</sup> A. Ferretti,<sup>1</sup> M. Floris,<sup>6</sup> A. Forster,<sup>2</sup> P. Force,<sup>4</sup> N. G. Uetzel,<sup>2,4</sup> A. Guichard,<sup>8</sup> H. Gulkanian,<sup>10</sup> J. M. Heuser,<sup>9</sup> M. Keil,<sup>2,7</sup> L. Kluberg,<sup>2,5</sup> C. Lourenco,<sup>2</sup> J. Lozano,<sup>7</sup> F. Manso,<sup>4</sup> P. Martinis,<sup>2,7</sup> A. Mazoni,<sup>6</sup> A. Neves,<sup>7</sup> H. Ohnishi,<sup>9</sup> C. Oddo,<sup>1</sup> P. Parracho,<sup>2</sup> P. Pillot,<sup>8</sup> T. Poghosyan,<sup>10</sup> G. Puudu,<sup>6</sup> E. Rademacher,<sup>2</sup> P. Ramalhete,<sup>2</sup> P. Rosinsky,<sup>2</sup> E. Scamporrino,<sup>1</sup> J. Seixas,<sup>7</sup> S. Serci,<sup>6</sup> R. Shahoyan,<sup>2,7</sup> P. Sonderegger,<sup>7</sup> H. J. Specht,<sup>3</sup> R. Teulent,<sup>8</sup> G. Urai,<sup>6</sup> R. Veenhof,<sup>2</sup> and H. K. W. Ohm,<sup>6,7</sup>

(NA60 Collaboration)

<sup>1</sup>Università di Torino and INFN, Italy

<sup>2</sup>CERN, 1211 Geneva 23, Switzerland

<sup>3</sup>Physikalisches Institut der Universität Heidelberg, Germany

<sup>4</sup>LPC, Université Blaise Pascal and CNRS-IN2P3, Clermont-Ferrand, France

<sup>5</sup>LLR, Ecole Polytechnique and CNRS-IN2P3, Palaiseau, France

<sup>6</sup>Università di Cagliari and INFN, Cagliari, Italy

<sup>7</sup>Instituto Superior Técnico, Lisbon, Portugal

<sup>8</sup>IPN-Lyon, Université Claude Bernard Lyon-I and CNRS-IN2P3, Lyon, France

<sup>9</sup>RIKEN, Wako, Saitama, Japan

<sup>10</sup>YerPhI, Yerevan Physics Institute, Yerevan, Armenia

(Dated: June 8, 2013)

The NA60 experiment at the CERN SPS has studied dimuon production in 158A GeV In-In collisions. The strong excess of pairs above the known sources found in the complete mass region  $0.2 < M < 2.6$  GeV has previously been interpreted as thermal radiation. We now present first results on the associated angular distributions. Using the Collins-Soper reference frame, the structure function parameters  $A$ ,  $B$ , and  $C$  are measured to be zero, and the projected distributions in polar and azimuthal angles are found to be uniform. The absence of any polarization is consistent with the interpretation of the excess dimuons as thermal radiation from a randomized system.

Lepton pairs are a particularly attractive observable to study the hot and dense matter created in high-energy nuclear collisions. Their continuous emission, undisturbed by final-state interactions, probes the entire space-time evolution of the rebell, including the early phases with the conjectured QCD phase transitions of chiral symmetry restoration and parton deconfinement. To the extent that the bulk constituents of the expanding matter (hadrons and partons) equilibrate, the direct lepton pairs generated by them are commonly referred to as 'thermal radiation'. Our previous work has indicated 'thermal' dilepton production to be largely mediated for  $M < 1$  GeV by  $\pi^+\pi^-$  annihilation via the strongly broadened vector meson  $\rho(770)$ , and for  $M > 1$  GeV by partonic processes like  $q\bar{q}$  annihilation [2, 3]. The two dilepton variables basically explored in this work were mass  $M$  and transverse momentum  $p_T$ , where the correlations between the two were decisive in bearing out the nature of the emission sources in the two mass regions [2, 3].

Further information on the production mechanism and the distribution of the annihilating particles, complementary to that from  $M$  and  $p_T$ , can be obtained from the study of dilepton angular distributions. This Letter presents the first measurement of full dilepton angular distributions in the field of high-energy nuclear collisions. It is restricted to the mass region  $M < 1$  GeV, due to the lack of sufficient statistics for  $M > 1$  GeV. The question asked is simple: can one get direct experimental insight

into whether the radiating matter is thermalized?

Historically, the interest in angular distributions of continuum lepton pairs was mostly motivated by the study of the Drell-Yan mechanism, following in particular the insight that the 'naive' QED interpretation [1] had to be significantly modified due to QCD effects [5, 6, 7, 8]. The differential decay angular distribution in the rest frame of the virtual photon with respect to a suitably chosen set of axes, ignoring the rest mass of the leptons, can quite generally be written as

$$\frac{1}{d} \frac{d^2}{d\Omega d\cos\theta} \propto (1 + \cos^2\theta + \sin^2\theta \cos^2\phi + \frac{1}{2} \sin^2\theta \cos 2\phi) \quad (1)$$

The angular dependence on polar angle  $\theta$  and azimuthal angle  $\phi$  dates back to [9], but the specific coefficients  $A$ ,  $B$ , and  $C$ , the 'structure function' parameters, follow the nomenclature in e.g. [8, 10]. They are directly related to the helicity structure functions  $W_i$  defined in [6], and in particular to the spin density matrix  $R_{ij}$  of the virtual photon, the main object of the spin analysis [7, 10, 11]. We have chosen here the Collins-Soper (CS) reference frame [5], where the quantization axis  $z$  is defined as the bisector between the beam and negative target momenta  $\mathbf{p}_{\text{beam}}$  and  $\mathbf{p}_{\text{target}}$ , which define the reaction plane. The polar angle  $\theta$  is then the angle between the momentum of the positive muon  $\mathbf{p}_+$  and the  $z$  axis, which define the decay plane, while the azimuthal angle  $\phi$  is the angle between the reaction and the decay planes. However, the

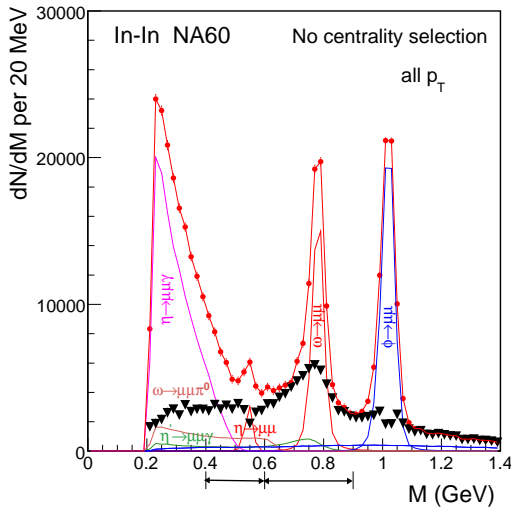


FIG. 1: Isolation of an excess above the electromagnetic decays of neutral mesons (see text). Total data (closed circles), individual cocktail sources (solid lines), difference data (thick triangles), sum of cocktail sources and difference data (line through the closed circles). Open charm still contained.

particular choice of the frame is not really relevant here, since the determination of the full set of coefficients  $\alpha$ ,  $\beta$  and  $\gamma$  allows to compute them in any other frame by a simple transformation [8]. This would not apply if only the  $\cos\theta$  distribution would be measured.

In principle, the dilepton angular distributions can be anisotropic, with all structure function parameters  $\alpha$ ;  $\beta$ ;  $\gamma$   $\in \mathbb{R}$  [5, 6, 7, 8, 10]. Even for spinless particles in the initial state like in  $e^+e^-$  annihilation, the parameters can still have any value  $\in \mathbb{R}$ , since the spin density matrix of the virtual photon also receives contributions from orbital angular momentum [12]. Very elementary examples are  $qq$  and  $e^+e^-$  annihilation along the beam direction for  $p_T = 0$ . Here  $\alpha = \beta = 0$  and  $\gamma = +1$  for  $qq$  (like lowest order DY [4]) and  $\gamma = 1$  for  $e^+e^-$  [12], corresponding to transverse and longitudinal polarization of the virtual photon, respectively. However, a completely random orientation of annihilating partons or pions in 3 dimensions (but not in 2 [11]) would lead to  $\alpha$ ;  $\beta$ ;  $\gamma = 0$  [11, 12, 13], and that is the case of prime interest here.

Details of the NA60 apparatus are contained in [3, 14]. The data sample for 158A GeV In-In collisions is the same as used in [1, 2], and the different analysis steps follow the same sequence: assessment of the combinatorial background from  $\pi$  and K decays by a mixed-event technique, assessment of the fake-matches (associations of muons to non-muon vertex tracks in the Sipixel telescope), isolation of the dimuon excess by subtraction of the known meson decay sources and charm from the net opposite-sign sample, and finally correction for acceptance and pair efficiency. All steps are now done independently in each  $[\frac{dN}{d\cos\theta} \frac{d}{d}]_{j_j}$  bin. The binning is varied depending on the goal, thereby assuring that the results

are stable with respect to the bin widths chosen.

The assessment of the two background sources and open charm is extensively discussed in the ref. [3]. The centrality-integrated net mass spectrum after background subtraction is shown in Fig. 1 together with the contributions from neutral meson decays: the 2-body decays of the  $\rho^0$ ,  $\omega$  and  $\eta$  resonances, and the Dalitz decays of the  $\rho^0$ ,  $\omega$  and  $\eta$ . The data clearly exceed the sum of the decay sources. The excess dimuons are isolated by subtracting them from the total (except for the  $\rho^0$ ), based solely on local criteria [1, 2]. The excess for  $M < 1$  GeV is interpreted as the strongly broadened  $\rho^0$  which is continuously regenerated by  $e^+e^-$  annihilation [1, 2]. Two adjacent mass windows indicated in Fig. 1 are used for the subsequent angular distribution analysis: the  $\rho^0$ -like region  $0.6 < M < 0.9$ , and the low-mass tail  $0.4 < M < 0.6$  GeV. To exclude the region of the low- $m_T$  rise seen for all masses [2], a transverse momentum cut of  $p_T > 0.6$  GeV is applied, leaving about 54000 excess pairs in the two mass windows. The subtracted data for the  $\rho^0$  and  $\omega$ , about 73000 pairs, are subject to the same further analysis steps as the excess data and are used for comparison.

The correction for the acceptance of the NA60 apparatus requires, in principle, a 5-dimensional grid in  $M - p_T - y - \cos\theta - \phi$  space. To avoid large statistical errors in low-acceptance bins, the correction is performed in 2-dim.  $\cos\theta - \phi$  space, using the measured data for  $M, p_T$  [2] and  $y$  [15] as an input to the Monte Carlo (MC) simulation of the  $\cos\theta - \phi$  acceptance matrix. The sensitivity of the final results to variations of this  $M - p_T - y$  input has been checked, and the effects are found to be considerably smaller than the statistical errors of the results. The MC simulations were done in an overlay mode with real data to include the effects of pair reconstruction efficiencies. The product acceptance efficiency is illustrated in

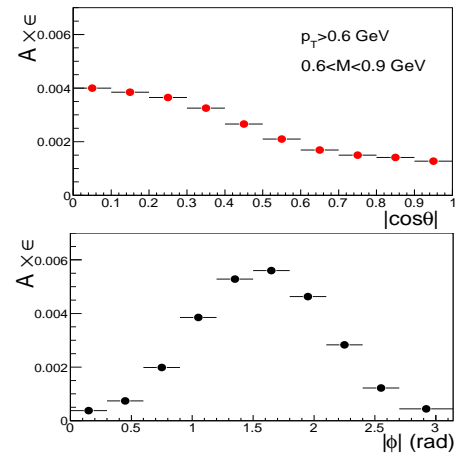


FIG. 2: Spectrometer acceptance as a function of the two angular variables  $|\cos\theta|$  and  $|\phi|$ .

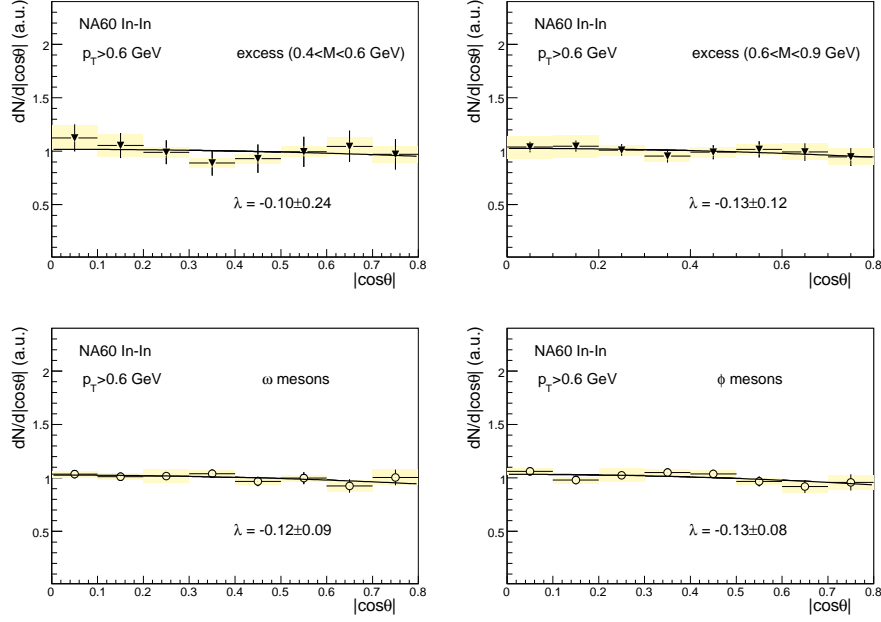


FIG. 3: Polar angle distributions of excess dileptons and of the vector mesons  $\omega$  and  $\phi$ .

Fig. 2 for  $0.6 < M < 0.9$  GeV and  $p_T > 0.6$  GeV. The rapidity coverage is  $3.2 < y < 4.2$  ( $+0.3 < y_{cm} < +1.3$ ).

The results on the angular distributions have been analysed in three different ways, distinguished by the method and the associated statistical/systematic errors. In the first and most rigorous method (1), the 3 structure function parameters  $A_0$ ,  $A_1$  and  $A_2$  are extracted from a simultaneous fit of the 2-dimensional data on the basis of Eq.(1), using a  $6 \times 6$  matrix in the range  $-0.6 < \cos \theta < +0.6$  (bin width 0.2) and  $-0.75 < \cos \theta < 0.75$  (bin width 0.25). The restrictions in range are enforced by regions of very low acceptance in the 2-dimensional acceptance matrix, masked in the projections of Fig. 2. The fit values are summarized in Table I for all 4 cases, the two excess mass windows, the  $\omega$  and the  $\phi$ . Within errors, they are all compatible with zero. It is reassuring to see that this is also true for  $\lambda$ , as expected for a symmetric collision system at midrapidity on the basis of symmetry considerations [11].

In the second method (2), setting now  $A_2 = 0$ , the 2-dimensional acceptance-corrected data are projected onto either the  $\cos \theta$  or the  $\theta$  axis, summing over the two signs. The polar angular distribution is obtained by integrating Eq.(1) over the azimuthal angle ( $\phi$ )

$$\frac{dN}{d\cos\theta} = A_0(1 + \cos^2\theta); \quad (2)$$

while the azimuthal angular distribution is obtained by integration over the polar angle ( $\cos \theta$ )

$$\frac{dN}{d\theta} = A_1\left(1 + \frac{2}{3} + \frac{1}{3}\cos 2\theta\right) \quad (3)$$

The structure function parameters  $A_0$  and  $A_1$  can then be determined independently by 1-dimensional fits to the respective projections. The data of the polar angular distributions together with the fit lines according to Eq.(2) are shown in Fig. 3 for all four cases, using now 8 bins in  $\cos \theta$  (bin width 0.1). The distributions are seen to be uniform, and the fit parameters  $A_0$  and  $A_1$ , included in Table I, are again compatible with zero, within errors. To determine the parameter  $\lambda$ , (contained in Eq.(3)) is set to the measured value of  $A_1/A_0$ . The fit results for  $\lambda$  on the basis of Eq.(3), keeping the same number of bins used in method 1, are again zero, within errors (see Table I).

In the third method (3), the inclusive measured distributions in  $\cos \theta$  and  $\theta$  are analysed. A 1-dimensional acceptance correction is applied in each case, determined by using (as now measured) uniform distributions in  $\theta$  (for  $\cos \theta$ ) and in  $\cos \theta$  (for  $\theta$ ) as an input to the MC simulations. The number of bins in  $\cos \theta$  is kept, while that in  $\theta$  is increased to 10 (bin width 0.3). The data for the azimuthal angular distributions together with the fit lines according to Eq.(3) are shown in Fig. 4. The distributions are again uniform, as are those for  $\cos \theta$  (not shown, since hardly distinguishable from Fig. 3). The resulting fit parameters for  $A_0$  and  $A_1$  (taking account again of  $A_2 = 0$ ) are included in Table I. As expected, the errors are smaller than for the other two methods, but the values of  $A_0$  and  $A_1$  are still close to zero, within errors.

Figs. 3 and 4 also contain the systematic errors attached to the individual data points. They mainly arise from two sources. The subtraction of the combinatorial background, with relative uncertainties of 1% [1, 2, 3],

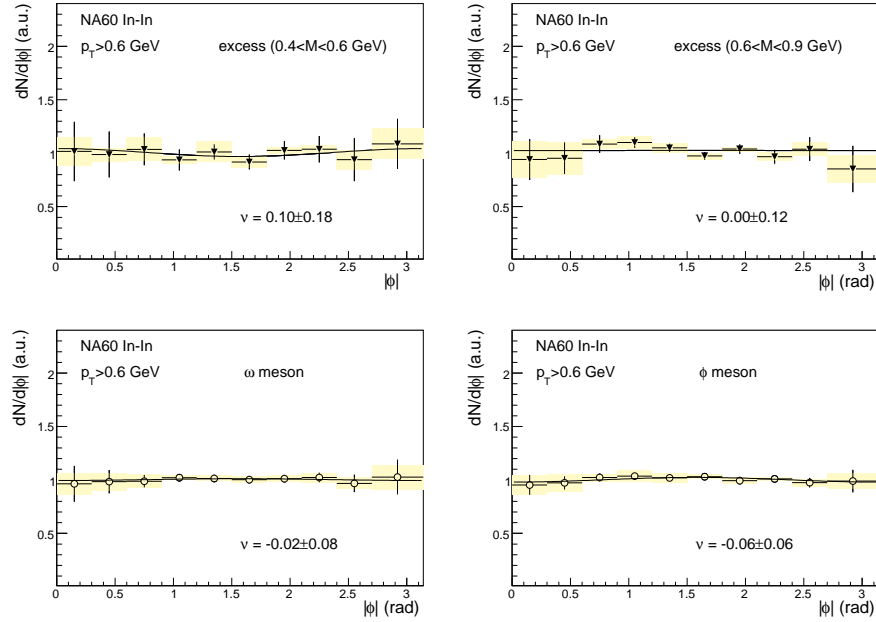


FIG. 4: Azimuthal angle distributions of excess dileptons and of the vector mesons  $\omega$  and  $\phi$ .

leads to errors of 2-3% of the net data for the kinematic selection used here. The subtraction of the meson decay sources causes (correlated) errors for the excess and the vector mesons  $\omega$  and  $\phi$ . With respect to the excess, they range from 4-6% up to 10-15% in the low-populated

TABLE I: Summary of results for  $p_T > 0.6$  GeV on the structure function parameters  $v$ , and  $\cos^2 - m$  matrix bins. The  $\chi^2_{\text{ndf}}$  of the fits varies between 0.8 and 1.2. For a cut  $p_T > 1.0$  GeV, the results are the same, within errors.

excess						
$0.6 < M < 0.9$ GeV						
method1	-0.19	0.12	0.03	0.15	0.05	0.03
method2	-0.13	0.12	0.05	0.15		
method3	-0.15	0.09	0.00	0.12		
excess						
$0.4 < M < 0.6$ GeV						
method1	-0.13	0.27	0.12	0.30	-0.04	0.10
method2	-0.10	0.24	0.11	0.30		
method3	-0.09	0.16	0.10	0.18		
$\omega$ meson						
method1	-0.10	0.10	-0.05	0.11	-0.05	0.02
method2	-0.12	0.09	-0.06	0.10		
method3	-0.12	0.06	-0.02	0.08		
$\phi$ meson						
method1	-0.07	0.09	-0.10	0.08	0.04	0.02
method2	-0.13	0.08	-0.09	0.08		
method3	-0.05	0.06	-0.06	0.06		

bins. This variation is well visible for the overall errors plotted in Figs. 3 and 4. Assuming, very conservatively, these errors to be uncorrelated from point to point, the (statistical) errors for  $v$  and  $\cos^2 - m$  quoted in Table I would increase by 15-20% if the systematic errors would be added in quadrature. Further confidence into the stability of the results is obtained from their independence of the methods and the bin widths used.

The global outcome from our analysis of dilepton angular distributions is straightforward: the structure function parameters  $v$ , and  $\cos^2 - m$  are all zero within the statistical and systematic errors, and the projected distributions in polar and azimuthal angle are all uniform. This applies not only for the excess dileptons as anticipated if of thermal origin, but also for the vector mesons  $\omega$  and  $\phi$ . While there may be a rather direct connection between the two findings in nuclear collisions, it is of interest to note that the result of  $v = 0$  has been reported before for  $\omega$  and  $\phi$  production in p-p [16] and  $^3\text{He}$ -C [17].

We conclude, following the primary motivation of this study, that the absence of any polarization is fully consistent with the interpretation of the observed excess dileptons as thermal radiation from a randomized system. While this is a necessary condition, it is not sufficient. However, together with other features like the Planck-like shape of the excess mass spectra [3, 18], the exponential shape of the  $m_T$  spectra [2, 18] and the global agreement with theoretical models both as to spectral shapes and absolute yields [3, 18], the thermal interpretation has become more plausible than ever before.

We are grateful to O. Nachtmann for useful discussions.

- 
- [1] R. A. Maki et al. (NA 60 Collaboration), *Phys. Rev. Lett.* **96**, 162302 (2006).
- [2] R. A. Maki et al. (NA 60 Collaboration), *Phys. Rev. Lett.* **100**, 022302 (2008).
- [3] R. A. Maki et al. (NA 60 Collaboration), *Eur. Phys. J.* (2009) in press; arXiv:0810.3204.
- [4] S. D. Drell and T. M. Yan, *Phys. Rev. Lett.* **25**, 316 (1970).
- [5] J. C. Collins and D. E. Soper, *Phys. Rev. D* **16**, 2219 (1977).
- [6] C. S. Lam and W. K. Tung, *Phys. Rev. D* **18**, 2447 (1978).
- [7] J. Badier et al. (NA 3 Collaboration), *Z. Phys. C* **11**, 195 (1981).
- [8] S. Falciano et al. (NA 10 Collaboration), *Z. Phys. C* **31**, 513 (1986) and M. Guanziroli et al. (NA 10 Collaboration), *Z. Phys. C* **37**, 545 (1988).
- [9] K. Gottfried and J. D. Jackson, *Nuovo Cim.* **33**, 309 (1964).
- [10] A. Brandenburg, O. Nachtmann and E. Mirkes, *Z. Phys. C* **60**, 697 (1993); D. Boer, A. Brandenburg, O. Nachtmann and A. Utermann, *Eur. Phys. J. C* **40**, 55 (2005).
- [11] O. Nachtmann, private communication (2008).
- [12] E. L. Bratkovskaya, O. V. Teryaev, V. D. Toneev, *Phys. Lett. B* **348**, 283 (1995).
- [13] P. Hoyer, *Phys. Lett. B* **187**, 162 (1987).
- [14] K. Banicz et al., *Nucl. Instrum. Meth. A* **546**, 51 (2005).
- [15] S. Damjanovic et al., *Nucl. Phys. A* **783**, 327 (2007).
- [16] V. Blobel et al., *Phys. Lett. B* **48**, 73 (1974).
- [17] J. G. Branson et al., *Phys. Rev. Lett.* **38**, 1331 (1977).
- [18] R. A. Maki et al. (NA 60 Collaboration), *Eur. Phys. J.* (2009) in press; arXiv:0812.3053